BNL 29826

CONF-811101--10

REVIEW OF MELTING AND EVAPORATION OF FUSION-REACTOR FIRST WALLS*†

J.A. Fillo and H. Makowitz
Department of Nuclear Energy
Brookhaven National Laboratory
Upton, New York 11973

MASTER

ABSTRACT

The most severe thermal loading on the first wall will occur when the plasma becomes unstable resulting in a hard plasma disruption or at the end of a discharge when the plasma is dumped on the wall in a very short period of time. Hard plasma disruptions are of particular concern in future fusion reactors where the thermal energy of the plasma may reach values on the order of 300 MJ. Sufficiently high heating rates can occur to melt the first wall surface, and the temperature can increase resulting in vaporization. Thermal models are reviewed which treat these problems.

DISCLAIMER

This book was prepared as an account of work sponsored by an agency of the United States Government. Neither the United States Government nor any agency thereof, nor any of their employees, makes any warranty, express or implied, or assumes any legal liability or responsibility for the accuracy, completeness, or usefulness of any information, apparatus, product, or process disclosed, or represents that its use would not infringe privately owned rights. Reference herein to any specific commercial product, process, or service by trade name, trademark, manufacturer, or otherwise, does not necessarily constitute or imply its endorsement, recommendation, or favoring by the United States Government or any agency thereof. The views and opinions of authors expressed herein do not necessarily state or reflect those of the United States Government or any agency thereof.

DISTRIBUTION OF THIS DOCUMENT IS UNLIMITED

A = Area of first wall subjected to disruption, cm^2.
c = Specific heat, W-sec/g°C.
h = Heat transfer coefficient at cooled surface, W/cm^2-°C.
k = Thermal conductivity, W/cm-°C.
L = Latent heat of melting, J/g.
ℓ = Slab thickness, cm (Fig. 1).
Q = Total energy deposited to first wall during disruption, J.
Q_o = Applied surface heat flux, W/cm^2.
S_o = Defined in Eq. (1), W/cm^3.
t = Time, sec.
T = Temperature, °C.
ΔH = Heat of evaporation, J/g.
γ = Defined by exponential in Eq. (1), cm^{-1}
κ = Thermal diffusivity, cm^2/sec.
ρ = Density, g/cm^3.
τ = Disruption time, ms.

Subscripts
f = Fluid.
m = Melting.
o = Initial time.
s = Solid.

*Work performed under the auspices of the U.S. Dept. of Energy, Washington, DC 20585
†By acceptance of this article, the publisher and/or recipient acknowledge the U.S. Government's right to retain a nonexclusive, royalty-free license in and to any copyright covering this paper.

INTRODUCTION

For a deuterium-tritium (D-T) plasma, a large fraction (~80%) of the fusion energy is released as ~14-MeV neutrons as well as charged particles and radiation. The neutrons must be slowed down in a relatively thick structure, commonly referred to as the blanket, which surrounds the plasma. The neutron kinetic energy is converted to high-temperature heat. As a consequence of the charged particles and radiation, the blanket surface interfacing the plasma or first wall is exposed to a high heat flux. The heating by neutrons and surface heat is continuously removed from the blanket by a coolant system which is converted to electricity in a standard thermal cycle, i.e., a steam or gas turbine cycle in the case of a power reactor. Since the thermodynamic efficiency of such a cycle is governed by the operating temperature of the heat source, the problems of heat removal from a fusion reactor are of considerable importance. In addition to being a good moderator of neutrons with sufficiently good heat transfer characteristics for efficient heat removal, the blanket must breed tritium from lithium for commercial power reactors.

The first wall appears foremost as the region of concern since all of the emissions from a reacting plasma may intersect this wall. These include ions and neutral particles, primary neutrons, x-rays (Bremsstrahlung), and cyclotron radiation. In addition, scattered neutrons and gamma radiation generated in the blanket regions exterior to the first wall are also imposed on it. Finally, D-T gas surrounding the plasma may react chemically with the first wall materials. One result of these many interactions is the generation of appreciable heat which can be up to 20% of the plasma output; thus provision must be included for adequate cooling. In most analyses, the above effects are lumped together as a radiant flux. While the incident fluxes are absorbed in a small depth of any first wall material, the assumption is to treat the lumped radiant flux as if it were deposited on the first wall surface. In heat transfer analyses, it is an applied heat flux boundary condition. The

phenomena of sputtering and blistering, the formation of gaseous reaction products, and material vaporization processes from the first wall may represent the major sources of impurity in the plasma. Thus, the first wall can be a limiting component in the reactor power output due to a large power generation within it; and it may also limit plasma performance through impurity levels.

The most severe thermal loading on the first wall will occur when the plasma becomes unstable resulting in a hard plasma disruption or at the end of a discharge when the plasma is dumped on the wall in a very short period of time. Hard plasma disruptions are of particular concern in future fusion reactors where the thermal energy of the plasma may reach values on the order of 300 MJ for the INTOR design. Assuming a sufficiently high heating rate to melt the first wall surface, and if the temperature increases resulting in vaporization, a phase change problem arises. If the melted material is sloughed off the surface as it is formed, the moving boundary becomes the receding surface of the wall. If the melted meterial stays in place and reaches the boiling tempereture, a moving face where vaporization occurs becomes a boundary in addition to the moving internal boundary between the liquid and the solid. Because of the moving boundaries and the differences between the properties of the liquid and solid states of the same material, the temperature distribution is nonlinear.

Prior to a disruption approximately half of the total plasma energy content is plasma thermal energy and half is stored magnetic energy. During the disruption process, perhaps half of the stored magnetic energy is transformed into plasma thermal energy and then dissipated in the form of electromagnetic radiation or particle kinetic energy. The mechanism for energy transfer to the wall is highly dependent upon the plasma condition. Where the plasma is relatively "dirty," i.e., contains a high level of impurities, essentially all of the plasma energy will be transferred to the wall in the form of electromagnetic radiation. With this mechanism the energy is transferred to all of the first wall surfaces in essentially a uniform distribution. If the plasma is very "clean," however, essentially all of the energy will be transferred to the walls in the form of kinetic energy of plasma particles. Presumably, the real condition in the reactor will be somewhere between the "dirty" condition and the "clean" condition with some of the energy being transported by both mechanisms. The vaporization and melting of the first wall can effect the conditions of the local plasma, and the mode of energy transfer from the plasma to the wall.

For example, Sestero[1] has postulated that if during the early phase of the disruption the first wall begins to vaporize and the vapor penetrates the cold plasma edge, the first wall may be screened from the hot plasma interior by the colder plasma edge. Further wall erosion would be prevented. The ability of the edge plasma to absorb energy would be increased, and as the disruption proceeds, the vaporized material would spread out. This clearly implies that, in addition to heat conduction and phase change at the first wall, the dynamics of vapor transport need to be studied and coupled to the equation of motion and energy governing the plasma. This has yet to be done. The local magnetic field, its magnitude, direction, and gradients, can also effect the plasma/wall energy transfer.

The majority of thermal analyses which have modelled heat transfer in first walls due to plasma energy disruptions have assumed a uniform heat flux to the inboard wall of the reactor for the length of the plasma disruption. The assumption of uniform heat flux spreadout over the chamber wall seems reasonable if the mode of energy transport is in the form of radiation. Otherwise, the heat flux should rise rapidly to a much higher maximum than the radiation case, followed by an exponential decay over a much smaller first wall region. This case does not seem to have been analyzed. Thermal models for which analyses have been performed may be categorized as follows: (a) melting of a solid with melt layer in place;[2] (b) melting of a solid with complete removal of melt (ablation);[3] (c) melting/vaporization of the solid;[4,5] and (d) vaporization of the solid but no phase change affecting the temperature profile.[6]

In the latter case, the entire incident energy is conducted into the first wall, giving rise to a transient surface temperature. The amount of material vaporized is calculated separately based on the saturation vapor pressure. In ref. 2, the first wall is allowed to melt, and the amount of material vaporized is calculated separately as in the previous case. Melting and vaporization of the first wall has been coupled to a model for the dynamics of vapor transport using the computer code, RELAP-V.[7] This model needs further study, though, in particular the assumptions that were employed and constraints built into the program.

There is great uncertainty as to the time scale for plasma disruptions. For example, estimates range from 1 ms to possibly 100 ms, and in some cases, less than a millisecond. This impacts significantly as to whether melting and/or vaporization will dominate during a disruption. Coupled with other uncertainties, e.g., mode of plasma energy transport during the disruption, the plasma impact area, and the degree of uniformity of the impact, the conclusions drawn from heat transfer analyses point to the severity of a thermal problem for a given set of plasma assumptions.

FIRST WALL MODEL--PHYSICAL DESCRIPTION

The first wall concept is a relatively thick, ~2 cm or so, structure facing the plasma. This structure is essentially a thermal mass with cooling tubes welded or brazed to the rear surface (away from the plasma). Three objectives for having the thick wall are: (1) to protect the cooling tubes from off-normal energy dumps due to plasma disruptions or thermal transients; (2) for short pulse lengths, the thermal mass can significantly reduce the thermal fluctuations seen by the cooling tubes, reducing the alternating component of thermal stress, thereby giving a longer fatigue lifetime; and (3) in anticipation of high fluxes of charge exchange neutrals to the first wall substantial erosion of the first wall by sputtering appears likely.

The first wall is approximated by a slab geometry (Figure 1), the surface interfacing the plasma subjected to an applied heat flux (Bremsstrahlung energy, etc.), while the rear surface is convectively cooled.

Volumetric heating is due to neutron and gamma energy. While steady-state analyses yield the maximum temperatures, there are a wide range of time-dependent conditions which are anticipated. For example, in the case of steady-state commercial power reactors (long plasma burn), the dominant mode of temperature behavior will be steady state. In contrast, for expirimental or near-term reactors, plasma burn times may only be tens of seconds, with dwell times the same order of magnitude or greater, so that a

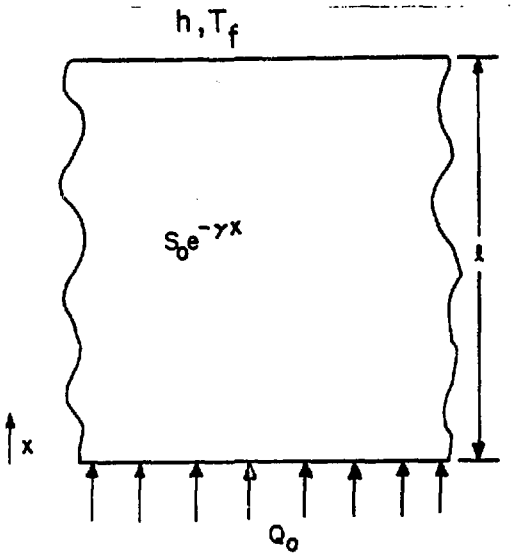

Fig. 1 One-dimensional slab geometry.

steady, periodic temperature behavior will persist.

Since the volumetric internal heat generation can be closely approximated by a decaying exponential function, the one-dimensional, time-dependent heat conduction equation may be written as:

$$\kappa \frac{\partial^2 T}{\partial x^2} - \frac{\partial T}{\partial t} = -\frac{S_o}{\rho c} e^{-\gamma x} \phi(t) \qquad (1)$$

subject to the following boundary and initial conditions,

$$-k \frac{\partial T}{\partial x} = Q_o \phi(t), \; x = 0; \; -k \frac{\partial T}{\partial x} = h(T - T_f), \; x = \ell \; , \qquad (2a)$$

and

$$T = T_o, \; t = 0 \quad . \qquad (2b)$$

Here, T is the temperature while S_o and γ are parameters dependent on plasma conditions as well as blanket structural material and are derived from the results of a neutronics analysis. Q_o is the incident flux to the first wall and is assumed to be a certain percentage of the plasma output, usually of the order of 20%. The heat transfer coefficient, h, and the mean fluid temperature, T_f, are assumed known. We assume the blanket structure is at some temperature, T_o, at time t=0.

The applied flux, $Q_o \phi(t)$, represents a flux, Q_o, which is "on" for time, $\tau_1(\phi(t)=1)$ and "off" for time, $\tau-\tau_1(\phi(t)=0)$ with period, τ. The general solution to Eq. (1), subject to Eqs. (2a,b) and the above flux, is given in ref. 8, and will not be repeated here.

Suddenly, a plasma disruption occurs, and the front face of the first wall is exposed to a uniform burst of radiant energy, Q, which is deposited on the inboard first wall area during a time interval, τ. The disruption is assumed to be initiated during the period when first wall temperatures reach steady state.

Given the above assumptions about the mode of plasma energy transport and the area over which the energy is deposited, the first wall thermal response is a function of the time scale for plasma disruption, the forces acting on the first wall during the disruption, and the plasma/wall interaction itself.

For example, if the slab is heated to the melting point, T_m, and the melted material is not sloughed off, vaporization can ensue. Another possibility is that the melted material is ablated. At this point, we are not in a position to say in a definitive say which case or cases do or will occur as a function of the plasma/wall interaction. Consequently, several mechanisms have been postulated and their consequences analyzed.

In either the region of melted material or in the solid material, the temperature distribution is adequately described by the heat conduction equation, Eq. (1), with appropriate constant local values for the thermal conductivity, specific heat, and density. The neutron and gamma heating source term is a second order effect since surface heating dominates, and has been neglected in plasma disruption analyses.

Case A: Melting of a solid.

In the general problem of melting of a solid, there exists a temperature distribution in both the liquid and solid phases. A constant heat flux, q, is applied for a short period of time, τ, at one face of a finite slab which is initially at some uniform temperature below the melting point; the other face of the slab is at its initial temperature. Eventually, the slab begins to melt. The problem is to determine how the melting propagates and how the temperature is distributed in the melted and unmelted portions of the slab.

During the rise time to the melting temperature, the heat transfer in the first wall is conduction or diffusion limited. If no phase change occurs, to calculate the surface temperature at the heated face and rise time, the slope of the first wall surface temperature matches the energy input according to:

$$-k' \frac{\partial T}{\partial x} = q = \frac{Q}{\tau A} \; , \; x=0 \quad . \qquad (3)$$

While the slab is finite, we may treat it as a semi-infinite solid during its early moments of heating. Solving Eq. (1), subject to the boundary conditions, Eq. (3), the temperature history is given by:[9]

$$T - T_o = \frac{2Q}{\tau A} \sqrt{\kappa t} \; \text{ierfc} \frac{x}{2\sqrt{\kappa t}} \; , \qquad (4)$$

where T_o, assumed uniform throughout at the maximum steady-state value, represents the slab temperature at t=0.

The surface temperature rise at x=0 for any t is simply:

$$T_s - T_o = \frac{2Q}{A\tau} \sqrt{\frac{\kappa t}{\pi}} \quad . \qquad (5)$$

To calculate the rise time to melting, we set, $T_s = T_m$, $t = t_m$, so that:

$$t_m = \frac{\pi}{\kappa} \left(\frac{T_m - T_o}{\frac{2Q}{A\tau}} \right)^2 \quad . \qquad (6)$$

At time, $t=t_m$, the surface temperature has risen to the melting temperature and the phase change ensues.

At any instant after melting starts, the slab consists of distinct liquid and solid portions containing melted and unmelted material (see Figure 2). The

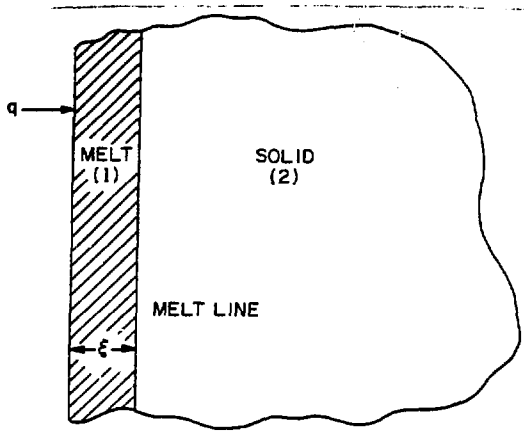

Fig. 2 Schematic representation of melting problem.

interface or melt line between these two regions, is specified by the function, $\xi(t)$ which gives the thickness of the liquid region at time, t. The problem is to determine the thickness of melt and the temperature distribution in the liquid and solid region, so as to satisfy the heat conduction equation in both regions, as well as the boundary conditions:

$$k_1 \frac{\partial T_1}{\partial x}\bigg|_{\xi} - k_2 \frac{\partial T_2}{\partial x}\bigg|_{\xi} = -\rho L_m \frac{d\xi}{dt} \quad , \tag{7}$$

$$T_1(\xi,t) = T_2(\xi,t) = T_m \quad , \text{ and} \tag{8}$$

$$\xi(o) = 0 \quad . \tag{9}$$

The subscripts 1 and 2 refer to the melted and solid regions, respectively. In addition to conditions (7) and (8), Eq. (3) must also be satisfied at x=0 for $t>t_m$ as well.

The general solution to Eq. (1), subject to Eqs. (3), (7), and (8), has been treated by the approximate integral method,[10] and more recently, by series solution.[11] Neither case treats, though, a pulsed heat source so that the approximate integral method and series solution need to be reworked to allow for cool down after the plasma disruption.

In ref. 2, ensuing melting and melting of the first wall has been calculated using the finite difference code, HEATING-V.[12] While the analysis for the rise time given by Eq. (6) is not used in HEATING-V, it nevertheless, gives the same results as HEATING-V.

Transient heat response during plasma disruptions has been analyzed for the projected surface heat loads, listed in Table 1. The corresponding maximum surface temperatures are also listed. Figure 3 indicates first wall surface temperature, as a function of time. The calculations account for the latent heat of fusion of the aluminum structure. For the projected surface heat load of 25,000 W/cm^2 applied for 10 msec, the peak surface temperature reached 1350°C, with a melting of the top 0.03 cm during the disruption (Figure 4). The surface fully solidifies within 10 msec after the end of the disruption.

TABLE 1--PROJECTED SURFACE HEAT LOADS AND MAXIMUM SURFACE TEMPERATURE DUE TO PLASMA DISRUPTIONS

Time, ms	10,500* W/cm^2	12,500 W/cm^2	25,000 W/cm^2
5			950°C
10			1350°C
20	850°C	1000°C	

*Average energy flux = 210 J/cm^2.

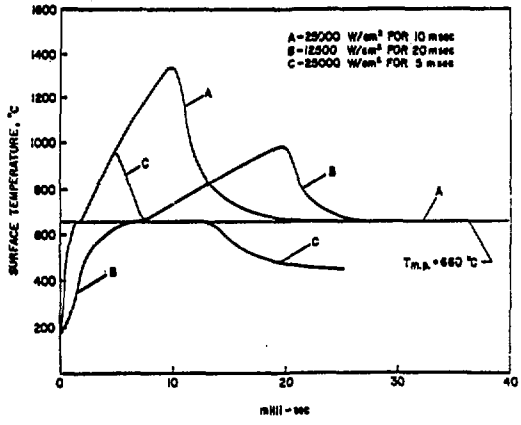

Fig. 3 First-wall surface temperature as a function of time.

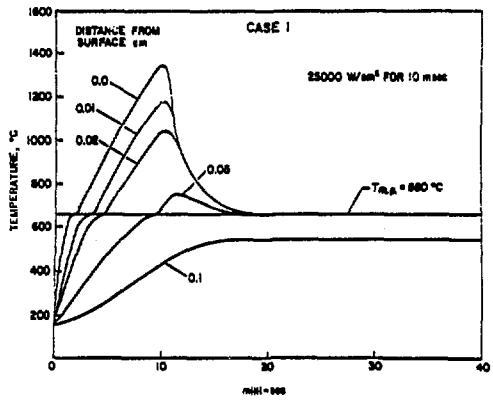

Fig. 4 Temperature distribution inside aluminum first wall.

When a solid is heated to a temperature well above 0 K, some of the atoms that are in the high energy tail of the thermal energy distribution will have sufficient energy to overcome the surface binding energy. If the momentum of these atoms at the surface is directed away from the surface, they will evaporate. Evaporation rates, dn/dt, from a surface at temperature, T_s, can generally be estimated from the equilibrium vapor pressure, p, of the solid material:[6]

$$\frac{dn}{dt} = \tilde{\alpha} \frac{3.5\times10^{22}}{\sqrt{m}} \frac{P(T_s)}{\sqrt{T_s}} \quad , \tag{10}$$

where $\tilde{\alpha}$ is the probability that an atom from the gas phase sticks at the surface (generally, $\tilde{\alpha}$=1), p is the vapor pressure, M is the mass number, and T_s is the surface temperature. Vapor pressure curves for metals may be described by:

$$P = P_o \exp(\Delta H/k_B T) \quad , \tag{11}$$

where ΔH is the heat of evaporation when the surface layer is melted. For a solid surface, ΔH is the heat of sublimation. The Boltzman constant is k_B.

Assuming the Behrisch model,[6] Eq. (10), for vaporization losses are ~3 μg/cm^2 during a disruption. About 10^3 disruptions are expected during the 10^6 pulse lifetime of INTOR[13] (6.6 MW(th) yr/m^2), so that the total vaporization loss is insignificant for this condition. Higher heat fluxes would, of course, result in larger vaporization losses. Lower thermal conductivity materials, such as stainless steel, appear to have much higher vaporization loss rates.

With regard to the thermal analysis, the open question is what happens to the melt layer formed during the disruption? Should the melt layer be removed by the magnetic pressure as produced by eddy currents in the wall during the disruption, the actual erosion rate for aluminum would be greater than the rate due to evaporation. An analysis of this case is made in the next Section.

Recent results from PLT[14] and the Doublet experiments[15] tend to show melting with some erosion followed by resolidification on limiters.

Case B: Melting of a solid with complete removal of melt (ablation).

If the melting liquid is completely removed as it is formed, as in the process of ablation, the surface recedes with time, the surface temperature remains constant at the phase-change temperature, and a temperature distribution exists only in the remaining solid, Figure 5.

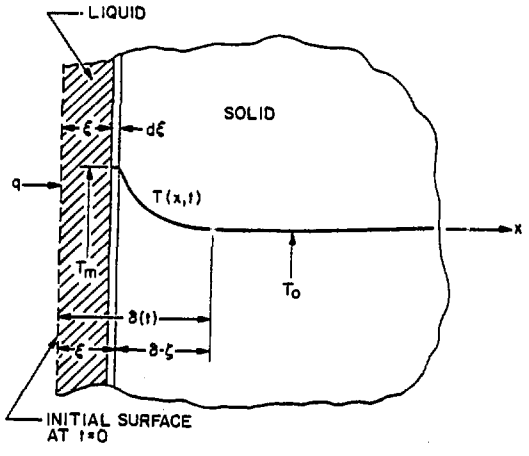

Fig. 5 Melting solid with complete removal of melt.

To analyze this problem, we assume that a semi-infinite solid is heated by sudden application of a constant heat flux, q, to the surface, x=0. At time, t=0, the first wall surface temperature is at the steady-state value. As time progresses, the surface temperature rises to the melting temperature. During this rise time, the heat transfer in the first wall is conduction-limited and can be calculated as previously discussed. As phase change ensues, the melted material is removed; thus, the boundary of the solid and the melt time are identical and located at x=ξ(t). The temperature distribution in the solid penetrates to a depth δ(t). The temperature for x>δ(t) is the constant T_o.

The heat balance at the melting face is:

$$q + k \frac{\partial T}{\partial x} = \rho L_m \frac{d\xi}{dt} \quad , \; x=\xi(t), \quad t>0, \tag{12}$$

where L_m is the latent heat of melting, all properties are referred to solid at the melting point. The constant heat flux, q=Q/τA, represents the heat flow into the solid with total energy, Q, dumped on an area, A, in time, τ.

The general solution to Eq. (1), subject to Eq. (12), has been treated by the approximate integral method, but not for a pulsed heat source. The specific application to the plasma disruption problem has been studied in ref. 3. The Grumman Q-Star ablation program was used to perform the analysis. The program is based on one-dimensional conduction with a moving boundary.

Figures 6 and 7 show the thermal responses of aluminum and stainless steel for representative plasma heat loads and plasma dump times. The curves labelled nodes 1, 2, etc., refer to the initial location of these nodes. As energy is supplied to the front surface of the first wall and melting ensues, the cells containing these modes loss mass giving rise to the irregular shape of the temperature curves. In other

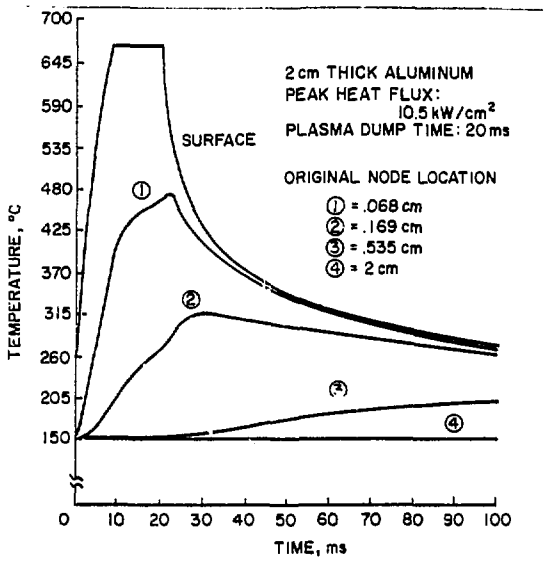

Fig. 6

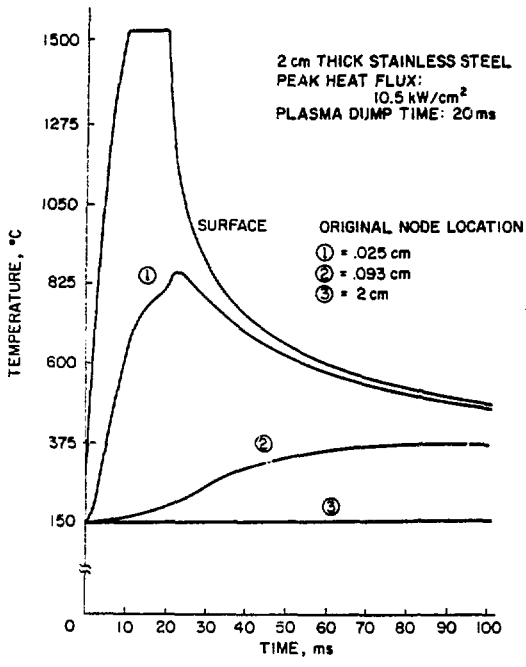

Fig. 7

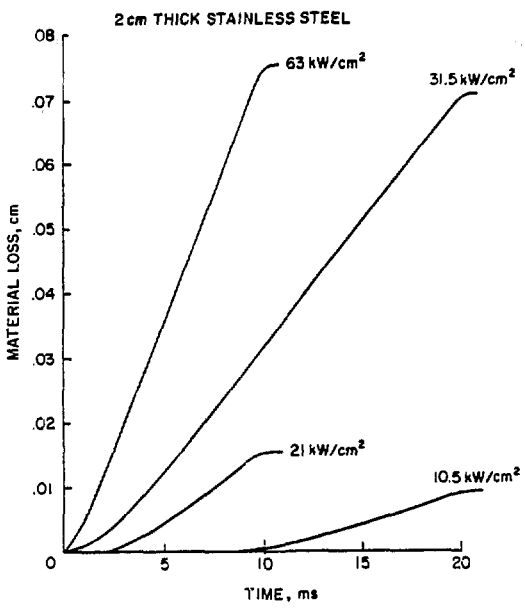

Fig. 9 Material loss due to disruption.

words, as material is lost during melting, a given cell does not contain the same material that it contained at time equal zero.

Figures 8 and 9 give the material loss of the first wall as a function of disruption time for Al and stainless steel under various heat flux loading conditions. For low heat fluxes and short disruption times, e.g., 10 kW/cm^2 and disruption times up to 10 ms, virtually no material is lost from the first wall for either stainless steel or aluminum materials. As the heat flux increases and/or the disruption time increases from time equal to zero significantly more material is depleted from the first wall.

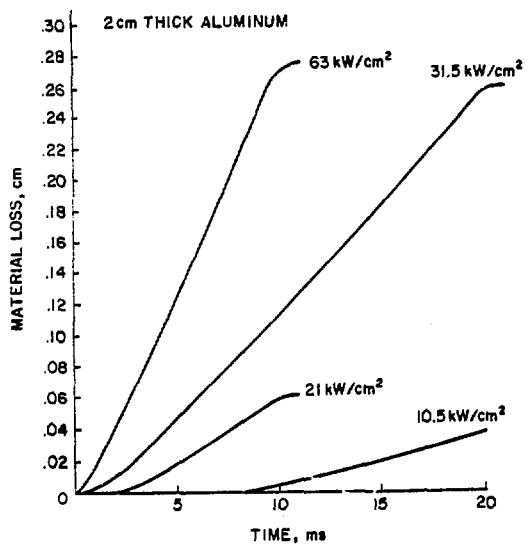

Fig. 8 Material loss due to disruption.

While aluminum tends to show significantly more material ablated than stainless steel at the higher heat flux, the 2-cm thick stainless steel wall is unrealistic. The stainless wall will be restricted to a maximum of 1 cm or less due to thermal stress considerations in realistic designs. Consequently, the material ablated from the stainless steel can also become significant for a thinner wall structure.

The ablation model is the most severe from the standpoint of material lost from the first wall during a disruption. Since the PLT and Doublet results tend to show melting followed by solidification on limiters, the question as to whether or not the extreme ablative case indicated here will be observed in future machines or experiments requires more tests on fusion devices during disruptive periods.

Case C: Melting and vaporization of a solid.

In this case, the melt stays in place and the temperature of one heated surface reaches the boiling temperature. As a result of the heating process, a moving boundary is formed between the liquid and solid regions and the receding face of the slab is at the boiling temperature. In the general problem of melting and vaporization, there exists a temperature distribution in both the liquid and the solid phase.

To analyze this problem, as in the previous case, we assume that the slab is heated by the suddan application of a constant heat flux, q, to the surface, x=0. At time, t=0, the first wall temperature is at

steady state. As time progresses, the surface temperature rises to the melting temperature, and the phase change ensues. The melted material remains in place until it reaches the boiling temperature, at which point the vaporized material leaves the surface. The boundary between the liquid region and the solid region moves at a rate designated by $d\xi/dt$. The conditions at the melt line, x=b, are designated by:

$$T_1(b,t) = T_2(b,t) \quad , \tag{13}$$

and

$$-k_1 \left.\frac{\partial T_1}{\partial x}\right|_b + k_2 \left.\frac{\partial T_2}{\partial x}\right|_b = L_m \rho \frac{d\xi}{dt} \quad , \tag{14}$$

where the subscripts 1 and 2 refer to the melt and solid regions, respectively.

When vaporization occurs at the surface, x=0, which is moving at a position, x=a, the boundary condition is:

$$q + k_1 \left.\frac{\partial T_1}{\partial x}\right|_a = L_v \rho \frac{d\eta}{dt} \quad , \tag{15}$$

where $d\eta/dt$ is the velocity with which the surface is receding as it vaporizes. The heat conduction equation, Eq. (1), must be solved in both the liquid and the solid regions.

Variants of this scenario and simplification to the general problem may be envisaged. For example, for materials of interest such as aluminum and stainless steel, the ratio of the latent heats of fusion and evaporization is so small compared with unit, so that the discontinuity at the melting boundary can be ignored to a good approximation. In essence, this removes the coupling between the melt and solid regions. The solid is assumed to be at the melting temperature and the vapor is immediately removed. Thus, a temperature distribution exists only in the liquid phase. The maximum rate of vaporization from a material is simply proportional to the surface heat flux. There is an initial pre-heating time before the surface starts to evaporate which for any given material depends upon the surface heat flux (according to an inverse square law). Solutions are found by using a perturbation expansion, the expansion parameter, ε, being the ratio of the heat loss by conduction to that by evaporation, i.e., $\varepsilon = \bar{c}T_v/L_v$, where $\bar{c}$ is the average value of the specific heat over the range $(0,T_v)$. This analysis has been applied to a plasma disruption problem in ref. 16.

In ref. 5, it is assumed that the plasma energy deposition time is short enough (milliseconds) and the depth of the affected region is so small (tens of micrometers) that only vaporization of the steel is important. Significant transport of metal in the liquid phase is not considered for the thin regions and short dump times of interest.

SUMMARY

A description of the plasma disruption problem and potential consequences to the first wall is made. In spite of the uncertainties in parameters such as plasma disruption time, magnitude of energy deposited, and disruption area (and mode of energy transport), some estimates of the impact of these parameters on the severity of the problem is shown. A key unresolved question is what happens to the melt layer formed during a disruption. Depending on the assumptions used, significantly different results are arrived at as to the amount of material ablated or vaporized. High thermal conductivity materials such as aluminum would be preferable compared with stainless steel whose thermal conductivity is an order of magnitude lower if the melt layer is not a problem. Even if the melt layer is a problem, since thermal stress severely limits the thickness of the stainless steel first wall, a high thermal conductivity material may well be preferable. Volumetric heating of the first wall by neutrons and gamma rays are a second order effect so that the thermal response is dominated by the surface heat flux. In conclusion, the plasma disruption phenomenon can have a significant impact on the life time of the first wall in magnetically-confined fusion reactors. The assumptions one makes concerning the modes of energy transfer as well as the area, location, and physical effects such as loss-of-the-melt layer, can significantly effect the severity of the heat transfer results. Even if the plasma physics evolves to the point where future machines can be made to operate in regimes free of plasma instabilities, one must still consider other potential disruptive mechanisms. For example, a magnet transient may cause the plasma to disrupt, and deposit its energy on the first wall. Even if there are only a few disruptions during the life of future machines, the thermal response of the first wall is important as these results have shown.

REFERENCES

1 Sestero, A., Nucl. Fusion, 17 (1977) 115.
2 Fillo, J., USA INTOR/80-1, 1980.
3 Fixler, S. and Timlen, W., GAC Memorandum, ES-80-171, 1980.
4 Andrews, J.G. and Atthey, D.R., J. Inst. Maths. Applics., 15 (1975) 59.
5. Smith, D.L. and Charah, L., Proceedings of the 7th Symposium on Engineering Problems of Fusion Research, Part II, 1977.
6 Behrisch, R., Nucl. Fusion 12 (1972) 695.
7 Merrill, B., INTOR/NUC/81-2, 1981.
8 Fillo, J., Nucl. Engr. Des., 48 (1978) 330.
9 Carslaw, H.S. and Jaeger, J.C., Conduction of Heat in Solids, Oxford Press, 1959
10 Goodman, T.R. and Shea, J.J., Transactions ASME, 1960.
11 Tao, L.M., ZAMP, 30 (1979) 416.
12 Turner, W.D. and Crowell, J.S., HEATING-V, Oak Ridge National Laboratory Computer Center, 1975.
13 INTOR/NUC/81-2, 1981.
14 Cohen, S.A., et al., Nucl. Fusion, 21 (1981) 233.
15 Hopkins, G., Private communication.
16 Loepel, L.L. and Wolfer, W.G., UWFDM-370, 1980.